



Determination of spin and parity of $D_{(s)}^*$ mesons

BESIII Collaboration*



M. Ablikim^a, M.N. Achasov^{m,2}, P. Adlarson^{ca}, R. Aliberti^{ak}, A. Amoroso^{bx,bz}, M.R. An^{ao}, Q. An^{bu,bg}, Y. Bai^{bf}, O. Bakina^{al}, I. Balossino^{ae}, Y. Ban^{av,7}, V. Batozskaya^{a,at}, K. Begzsuren^{ah}, N. Berger^{ak}, M. Berlowski^{at}, M. Bertani^{ab}, D. Bettoni^{ae}, F. Bianchi^{bx,bz}, E. Bianco^{bx,bz}, J. Bloms^{br}, A. Bortone^{bx,bz}, I. Boyko^{al}, R.A. Briere^e, A. Brueggemann^{br}, H. Cai^{cb}, X. Cai^{a,bg}, A. Calcaterra^{ab}, G.F. Cao^{a,bm}, N. Cao^{a,bm}, S.A. Cetin^{bk}, J.F. Chang^{a,bg}, T.T. Chang^{cc}, W.L. Chang^{a,bm}, G.R. Che^{as}, G. Chelkov^{al,1}, C. Chen^{as}, Chao Chen^{bd}, G. Chen^a, H.S. Chen^{a,bm}, M.L. Chen^{a,bg,bm}, S.J. Chen^{ar}, S.M. Chen^{bj}, T. Chen^{a,bm}, X.R. Chen^{ag,bm}, X.T. Chen^{a,bm}, Y.B. Chen^{a,bg}, Y.Q. Chen^{aj}, Z.J. Chen^{y,8}, W.S. Cheng^{bz}, S.K. Choi^j, X. Chu^{as}, G. Cibinetto^{ae}, S.C. Coen^d, F. Cossio^{bz}, J.J. Cui^{ay}, H.L. Dai^{a,bg}, J.P. Dai^{ce}, A. Dbeyssi^s, R.E. de Boer^d, D. Dedovich^{al}, Z.Y. Deng^a, A. Denig^{ak}, I. Denysenko^{al}, M. Destefanis^{bx,bz}, F. De Mori^{bx,bz}, B. Ding^{bp,a}, X.X. Ding^{av,7}, Y. Ding^{aj}, Y. Ding^{ap}, J. Dong^{a,bg}, L.Y. Dong^{a,bm}, M.Y. Dong^{a,bg,bm}, X. Dong^{cb}, S.X. Du^{cg}, Z.H. Duan^{ar}, P. Egorov^{al,1}, Y.L. Fan^{cb}, J. Fang^{a,bg}, S.S. Fang^{a,bm}, W.X. Fang^a, Y. Fang^a, R. Farinelli^{ae}, L. Fava^{by,bz}, F. Feldbauer^d, G. Felici^{ab}, C.Q. Feng^{bu,bg}, J.H. Feng^{bh}, K. Fischer^{bs}, M. Fritsch^d, C. Fritzsch^{br}, C.D. Fu^a, Y.W. Fu^a, H. Gao^{bm}, Y.N. Gao^{av,7}, Yang Gao^{bu,bg}, S. Garbolino^{bz}, I. Garzia^{ae,af}, P.T. Ge^{cb}, Z.W. Ge^{ar}, C. Geng^{bh}, E.M. Gersabeck^{bq}, A. Gilman^{bs}, K. Goetzenⁿ, L. Gong^{ap}, W.X. Gong^{a,bg}, W. Gradl^{ak}, S. Gramigna^{ae,af}, M. Greco^{bx,bz}, M.H. Gu^{a,bg}, Y.T. Gu^p, C.Y. Guan^{a,bm}, Z.L. Guan^v, A.Q. Guo^{ag,bm}, L.B. Guo^{aq}, R.P. Guo^{ax}, Y.P. Guo^{i,6}, A. Guskov^{al,1}, X.T. H.^{a,bm}, W.Y. Han^{ao}, X.Q. Hao^t, F.A. Harris^{bo}, K.K. He^{bd}, K.L. He^{a,bm}, F.H. Heinsius^d, C.H. Heinz^{ak}, Y.K. Heng^{a,bg,bm}, C. Herold^{bi}, T. Holtmann^d, P.C. Hong^{i,6}, G.Y. Hou^{a,bm}, Y.R. Hou^{bm}, Z.L. Hou^a, H.M. Hu^{a,bm}, J.F. Hu^{be,9}, T. Hu^{a,bg,bm}, Y. Hu^a, G.S. Huang^{bu,bg}, K.X. Huang^{bh}, L.Q. Huang^{ag,bm}, X.T. Huang^{ay}, Y.P. Huang^a, T. Hussain^{bw}, N. Hüskens^{aa,ak}, W. Imoehl^{aa}, M. Irshad^{bu,bg}, J. Jackson^{aa}, S. Jaeger^d, S. Janchiv^{ah}, J.H. Jeong^j, Q. Ji^a, Q.P. Ji^t, X.B. Ji^{a,bm}, X.L. Ji^{a,bg}, Y.Y. Ji^{ay}, Z.K. Jia^{bu,bg}, P.C. Jiang^{av,7}, S.S. Jiang^{ao}, T.J. Jiang^q, X.S. Jiang^{a,bg,bm}, Y. Jiang^{bm}, J.B. Jiao^{ay}, Z. Jiao^w, S. Jin^{ar}, Y. Jin^{bp}, M.Q. Jing^{a,bm}, T. Johansson^{ca}, X. K.^a, S. Kabana^{ai}, N. Kalantar-Nayestanaki^{bn}, X.L. Kangⁱ,

* E-mail address: besiii-publications@ihep.ac.cn.

¹ Also at the Moscow Institute of Physics and Technology, Moscow 141700, Russia.

² Also at the Novosibirsk State University, Novosibirsk, 630090, Russia.

³ Also at the NRC "Kurchatov Institute", PNPI, 188300, Gatchina, Russia.

⁴ Also at Goethe University Frankfurt, 60323 Frankfurt am Main, Germany.

⁵ Also at Key Laboratory for Particle Physics, Astrophysics and Cosmology, Ministry of Education; Shanghai Key Laboratory for Particle Physics and Cosmology; Institute of Nuclear and Particle Physics, Shanghai 200240, People's Republic of China.

⁶ Also at Key Laboratory of Nuclear Physics and Ion-beam Application (MOE) and Institute of Modern Physics, Fudan University, Shanghai 200443, People's Republic of China.

⁷ Also at State Key Laboratory of Nuclear Physics and Technology, Peking University, Beijing 100871, People's Republic of China.

⁸ Also at School of Physics and Electronics, Hunan University, Changsha 410082, China.

⁹ Also at Guangdong Provincial Key Laboratory of Nuclear Science, Institute of Quantum Matter, South China Normal University, Guangzhou 510006, China.

¹⁰ Also at Frontiers Science Center for Rare Isotopes, Lanzhou University, Lanzhou 730000, People's Republic of China.

¹¹ Also at Lanzhou Center for Theoretical Physics, Lanzhou University, Lanzhou 730000, People's Republic of China.

¹² Also at the Department of Mathematical Sciences, IBA, Karachi 75270, Pakistan.

X.S. Kang ^{ap}, R. Kappert ^{bn}, M. Kavatsyuk ^{bn}, B.C. Ke ^{cg}, A. Khoukaz ^{br}, R. Kiuchi ^a,
 R. Kliemt ⁿ, L. Koch ^{am}, O.B. Kolcu ^{bk}, B. Kopf ^d, M. Kuessner ^d, A. Kupsc ^{at,ca}, W. Kühn ^{am},
 J.J. Lane ^{bq}, J.S. Lange ^{am}, P. Larin ^s, A. Lavanía ^z, L. Lavezzi ^{bx,bz}, T.T. Lei ^{bu,11}, Z.H. Lei ^{bu,bg},
 H. Leithoff ^{ak}, M. Lellmann ^{ak}, T. Lenz ^{ak}, C. Li ^{aw}, C. Li ^{as}, C.H. Li ^{ao}, Cheng Li ^{bu,bg}, D.M. Li ^{cg},
 F. Li ^{a,bg}, G. Li ^a, H. Li ^{bu,bg}, H.B. Li ^{a,bm}, H.J. Li ^t, H.N. Li ^{be,9}, Hui Li ^{as}, J.R. Li ^{bj}, J.S. Li ^{bh},
 J.W. Li ^{ay}, Ke Li ^a, L.J. Li ^{a,bm}, L.K. Li ^a, Lei Li ^c, M.H. Li ^{as}, P.R. Li ^{an,10,11}, S.X. Li ⁱ, T. Li ^{ay},
 W.D. Li ^{a,bm}, W.G. Li ^a, X.H. Li ^{bu,bg}, X.L. Li ^{ay}, Xiaoyu Li ^{a,bm}, Y.G. Li ^{av,7}, Z.J. Li ^{bh}, Z.X. Li ^p,
 Z.Y. Li ^{bh}, C. Liang ^{ar}, H. Liang ^{a,bm}, H. Liang ^{bu,bg}, H. Liang ^{aj}, Y.F. Liang ^{bc}, Y.T. Liang ^{ag,bm},
 G.R. Liao ^o, L.Z. Liao ^{ay}, J. Libby ^z, A. Limphirat ^{bi}, D.X. Lin ^{ag,bm}, T. Lin ^a, B.J. Liu ^a, B.X. Liu ^{cb},
 C. Liu ^{aj}, C.X. Liu ^a, D. Liu ^{s,bu}, F.H. Liu ^{bb}, Fang Liu ^a, Feng Liu ^f, G.M. Liu ^{be,9}, H. Liu ^{an,10,11},
 H.B. Liu ^p, H.M. Liu ^{a,bm}, Huanhuan Liu ^a, Huihui Liu ^u, J.B. Liu ^{bu,bg}, J.L. Liu ^{bv}, J.Y. Liu ^{a,bm},
 K. Liu ^a, K.Y. Liu ^{ap}, Ke Liu ^v, L. Liu ^{bu,bg}, L.C. Liu ^{as}, Lu Liu ^{as}, M.H. Liu ^{l,6}, P.L. Liu ^a, Q. Liu ^{bm},
 S.B. Liu ^{bu,bg}, T. Liu ^{l,6}, W.K. Liu ^{as}, W.M. Liu ^{bu,bg}, X. Liu ^{an,10,11}, Y. Liu ^{an,10,11}, Y.B. Liu ^{as},
 Z.A. Liu ^{a,bg,bm}, Z.Q. Liu ^{ay}, X.C. Lou ^{a,bg,bm}, F.X. Lu ^{bh}, H.J. Lu ^w, J.G. Lu ^{a,bg}, X.L. Lu ^a, Y. Lu ^g,
 Y.P. Lu ^{a,bg}, Z.H. Lu ^{a,bm}, C.L. Luo ^{aq}, M.X. Luo ^{cf}, T. Luo ^{l,6}, X.L. Luo ^{a,bg}, X.R. Lyu ^{bm}, Y.F. Lyu ^{as},
 F.C. Ma ^{ap}, H.L. Ma ^a, J.L. Ma ^{a,bm}, L.L. Ma ^{ay}, M.M. Ma ^{a,bm}, Q.M. Ma ^a, R.Q. Ma ^{a,bm},
 R.T. Ma ^{bm}, X.Y. Ma ^{a,bg}, Y. Ma ^{av,7}, F.E. Maas ^s, M. Maggiora ^{bx,bz}, S. Maldaner ^d, S. Malde ^{bs},
 A. Mangoni ^{ac}, Y.J. Mao ^{av,7}, Z.P. Mao ^a, S. Marcello ^{bx,bz}, Z.X. Meng ^{bp},
 J.G. Messchendorp ^{n,bn}, G. Mezzadri ^{ae}, H. Miao ^{a,bm}, T.J. Min ^{ar}, R.E. Mitchell ^{aa},
 X.H. Mo ^{a,bg,bm}, N.Yu. Muchnoi ^{m,2}, Y. Nefedov ^{al}, F. Nerling ^{s,4}, I.B. Nikolaev ^{m,2}, Z. Ning ^{a,bg},
 S. Nisar ^{k,12}, Y. Niu ^{ay}, S.L. Olsen ^{bm}, Q. Ouyang ^{a,bg,bm}, S. Pacetti ^{ac,ad}, X. Pan ^{bd}, Y. Pan ^{bf},
 A. Pathak ^{aj}, Y.P. Pei ^{bu,bg}, M. Pelizaeus ^d, H.P. Peng ^{bu,bg}, K. Peters ^{n,4}, J.L. Ping ^{aq},
 R.G. Ping ^{a,bm}, S. Plura ^{ak}, S. Pogodin ^{al}, V. Prasad ^{ai}, F.Z. Qi ^a, H. Qi ^{bu,bg}, H.R. Qi ^{bj}, M. Qi ^{ar},
 T.Y. Qi ^{l,6}, S. Qian ^{a,bg}, W.B. Qian ^{bm}, C.F. Qiao ^{bm}, J.J. Qin ^{bv}, L.Q. Qin ^o, X.P. Qin ^{l,6}, X.S. Qin ^{ay},
 Z.H. Qin ^{a,bg}, J.F. Qiu ^a, S.Q. Qu ^{bj}, C.F. Redmer ^{ak}, K.J. Ren ^{ao}, A. Rivetti ^{bz}, V. Rodin ^{bn},
 M. Rolo ^{bz}, G. Rong ^{a,bm}, Ch. Rosner ^s, S.N. Ruan ^{as}, N. Salone ^{at}, A. Sarantsev ^{al,3},
 Y. Schelhaas ^{ak}, K. Schoenning ^{ca}, M. Scodelaggio ^{ae,af}, K.Y. Shan ^{l,6}, W. Shan ^x, X.Y. Shan ^{bu,bg},
 J.F. Shangguan ^{bd}, L.G. Shao ^{a,bm}, M. Shao ^{bu,bg}, C.P. Shen ^{l,6}, H.F. Shen ^{a,bm}, W.H. Shen ^{bm},
 X.Y. Shen ^{a,bm}, B.A. Shi ^{bm}, H.C. Shi ^{bu,bg}, J.L. Shi ^l, J.Y. Shi ^a, Q.Q. Shi ^{bd}, R.S. Shi ^{a,bm},
 X. Shi ^{a,bg}, J.J. Song ^t, T.Z. Song ^{bh}, W.M. Song ^{aj,a}, Y.J. Song ^l, Y.X. Song ^{av,7}, S. Sosio ^{bx,bz},
 S. Spataro ^{bx,bz}, F. Stieler ^{ak}, Y.J. Su ^{bm}, G.B. Sun ^{cb}, G.X. Sun ^a, H. Sun ^{bm}, H.K. Sun ^a, J.F. Sun ^t,
 K. Sun ^{bj}, L. Sun ^{cb}, S.S. Sun ^{a,bm}, T. Sun ^{a,bm}, W.Y. Sun ^{aj}, Y. Sun ⁱ, Y.J. Sun ^{bu,bg}, Y.Z. Sun ^a,
 Z.T. Sun ^{ay}, Y.X. Tan ^{bu,bg}, C.J. Tang ^{bc}, G.Y. Tang ^a, J. Tang ^{bh}, Y.A. Tang ^{cb}, L.Y. Tao ^{bv},
 Q.T. Tao ^{y,8}, M. Tat ^{bs}, J.X. Teng ^{bu,bg}, V. Thoren ^{ca}, W.H. Tian ^{ba}, W.H. Tian ^{bh}, Y. Tian ^{ag,bm},
 Z.F. Tian ^{cb}, I. Uman ^{bl}, B. Wang ^a, B.L. Wang ^{bm}, Bo Wang ^{bu,bg}, C.W. Wang ^{ar}, D.Y. Wang ^{av,7},
 F. Wang ^{bv}, H.J. Wang ^{an,10,11}, H.P. Wang ^{a,bm}, K. Wang ^{a,bg}, L.L. Wang ^a, M. Wang ^{ay},
 Meng Wang ^{a,bm}, S. Wang ^{an,10,11}, S. Wang ^{l,6}, T. Wang ^{l,6}, T.J. Wang ^{as}, W. Wang ^{bh},
 W. Wang ^{bv}, W.H. Wang ^{cb}, W.P. Wang ^{bu,bg}, X. Wang ^{av,7}, X.F. Wang ^{an,10,11}, X.J. Wang ^{ao},
 X.L. Wang ^{l,6}, Y. Wang ^{bj}, Y.D. Wang ^{au}, Y.F. Wang ^{a,bg,bm}, Y.H. Wang ^{aw}, Y.N. Wang ^{au},
 Y.Q. Wang ^a, Yaqian Wang ^{r,a}, Yi Wang ^{bj}, Z. Wang ^{a,bg}, Z.L. Wang ^{bv}, Z.Y. Wang ^{a,bm},
 Ziyi Wang ^{bm}, D. Wei ^{bt}, D.H. Wei ^o, F. Weidner ^{br}, S.P. Wen ^a, C.W. Wenzel ^d, U. Wiedner ^d,
 G. Wilkinson ^{bs}, M. Wolke ^{ca}, L. Wollenberg ^d, C. Wu ^{ao}, J.F. Wu ^{a,bm}, L.H. Wu ^a, L.J. Wu ^{a,bm},
 X. Wu ^{l,6}, X.H. Wu ^{aj}, Y. Wu ^{bu}, Y.J. Wu ^{ag}, Z. Wu ^{a,bg}, L. Xia ^{bu,bg}, X.M. Xian ^{ao}, T. Xiang ^{av,7},
 D. Xiao ^{an,10,11}, G.Y. Xiao ^{ar}, H. Xiao ^{l,6}, S.Y. Xiao ^a, Y.L. Xiao ^{l,6}, Z.J. Xiao ^{aq}, C. Xie ^{ar},
 X.H. Xie ^{av,7}, Y. Xie ^{ay}, Y.G. Xie ^{a,bg}, Y.H. Xie ^f, Z.P. Xie ^{bu,bg}, T.Y. Xing ^{a,bm}, C.F. Xu ^{a,bm},
 C.J. Xu ^{bh}, G.F. Xu ^a, H.Y. Xu ^{bp}, Q.J. Xu ^q, W.L. Xu ^{bp}, X.P. Xu ^{bd}, Y.C. Xu ^{cd}, Z.P. Xu ^{ar}, F. Yan ^{l,6},
 L. Yan ^{l,6}, W.B. Yan ^{bu,bg}, W.C. Yan ^{cg}, X.Q. Yan ^a, H.J. Yang ^{az,5}, H.L. Yang ^{aj}, H.X. Yang ^a,
 Tao Yang ^a, Y. Yang ^{l,6}, Y.F. Yang ^{as}, Y.X. Yang ^{a,bm}, Yifan Yang ^{a,bm}, Z.W. Yang ^{an,10,11},
 M. Ye ^{a,bg}, M.H. Ye ^h, J.H. Yin ^a, Z.Y. You ^{bh}, B.X. Yu ^{a,bg,bm}, C.X. Yu ^{as}, G. Yu ^{a,bm}, T. Yu ^{bv},
 X.D. Yu ^{av,7}, C.Z. Yuan ^{a,bm}, L. Yuan ^b, S.C. Yuan ^a, X.Q. Yuan ^a, Y. Yuan ^{a,bm}, Z.Y. Yuan ^{bh},
 C.X. Yue ^{ao}, A.A. Zafar ^{bw}, F.R. Zeng ^{ay}, X. Zeng ^{l,6}, Y. Zeng ^{y,8}, Y.J. Zeng ^{a,bm}, X.Y. Zhai ^{aj},
 Y.H. Zhan ^{bh}, A.Q. Zhang ^{a,bm}, B.L. Zhang ^{a,bm}, B.X. Zhang ^a, D.H. Zhang ^{as}, G.Y. Zhang ^t,
 H. Zhang ^{bu}, H.H. Zhang ^{bh}, H.H. Zhang ^{aj}, H.Q. Zhang ^{a,bg,bm}, H.Y. Zhang ^{a,bg}, J.J. Zhang ^{ba},

J.L. Zhang^{cc}, J.Q. Zhang^{aq}, J.W. Zhang^{a,bg,bm}, J.X. Zhang^{an,10,11}, J.Y. Zhang^a, J.Z. Zhang^{a,bm},
 Jiawei Zhang^{a,bm}, L.M. Zhang^{bj}, L.Q. Zhang^{bh}, Lei Zhang^{ar}, P. Zhang^a, Q.Y. Zhang^{ao,cg},
 Shuihan Zhang^{a,bm}, Shulei Zhang^{y,8}, X.D. Zhang^{au}, X.M. Zhang^a, X.Y. Zhang^{bd},
 X.Y. Zhang^{ay}, Y. Zhang^{bs}, Y.T. Zhang^{cg}, Y.H. Zhang^{a,bg}, Yan Zhang^{bu,bg}, Yao Zhang^a,
 Z.H. Zhang^a, Z.L. Zhang^{aj}, Z.Y. Zhang^{cb}, Z.Y. Zhang^{as}, G. Zhao^a, J. Zhao^{ao}, J.Y. Zhao^{a,bm},
 J.Z. Zhao^{a,bg}, Lei Zhao^{bu,bg}, Ling Zhao^a, M.G. Zhao^{as}, S.J. Zhao^{cg}, Y.B. Zhao^{a,bg},
 Y.X. Zhao^{ag,bm}, Z.G. Zhao^{bu,bg}, A. Zhemchugov^{al,1}, B. Zheng^{bv}, J.P. Zheng^{a,bg},
 W.J. Zheng^{a,bm}, Y.H. Zheng^{bm}, B. Zhong^{aq}, X. Zhong^{bh}, H. Zhou^{ay}, L.P. Zhou^{a,bm},
 X. Zhou^{cb}, X.K. Zhou^f, X.R. Zhou^{bu,bg}, X.Y. Zhou^{ao}, Y.Z. Zhou^{l,6}, J. Zhu^{as}, K. Zhu^a,
 K.J. Zhu^{a,bg,bm}, L. Zhu^{aj}, L.X. Zhu^{bm}, S.H. Zhu^{bt}, S.Q. Zhu^{ar}, T.J. Zhu^{l,6}, W.J. Zhu^{l,6},
 Y.C. Zhu^{bu,bg}, Z.A. Zhu^{a,bm}, J.H. Zou^a, J. Zu^{bu,bg}

^a Institute of High Energy Physics, Beijing 100049, People's Republic of China

^b Beihang University, Beijing 100191, People's Republic of China

^c Beijing Institute of Petrochemical Technology, Beijing 102617, People's Republic of China

^d Bochum Ruhr-University, D-44780 Bochum, Germany

^e Carnegie Mellon University, Pittsburgh, PA 15213, USA

^f Central China Normal University, Wuhan 430079, People's Republic of China

^g Central South University, Changsha 410083, People's Republic of China

^h China Center of Advanced Science and Technology, Beijing 100190, People's Republic of China

ⁱ China University of Geosciences, Wuhan 430074, People's Republic of China

^j Chung-Ang University, Seoul, 06974, Republic of Korea

^k COMSATS University Islamabad, Lahore Campus, Defence Road, Off Raiwind Road, 54000 Lahore, Pakistan

^l Fudan University, Shanghai 200433, People's Republic of China

^m G.I. Budker Institute of Nuclear Physics SB RAS (BINP), Novosibirsk 630090, Russia

ⁿ GSI Helmholtzcentre for Heavy Ion Research GmbH, D-64291 Darmstadt, Germany

^o Guangxi Normal University, Guilin 541004, People's Republic of China

^p Guangxi University, Nanning 530004, People's Republic of China

^q Hangzhou Normal University, Hangzhou 310036, People's Republic of China

^r Hebei University, Baoding 071002, People's Republic of China

^s Helmholtz Institute Mainz, Staudinger Weg 18, D-55099 Mainz, Germany

^t Henan Normal University, Xinxiang 453007, People's Republic of China

^u Henan University of Science and Technology, Luoyang 471003, People's Republic of China

^v Henan University of Technology, Zhengzhou 450001, People's Republic of China

^w Huangshan College, Huangshan 245000, People's Republic of China

^x Hunan Normal University, Changsha 410081, People's Republic of China

^y Hunan University, Changsha 410082, People's Republic of China

^z Indian Institute of Technology Madras, Chennai 600036, India

^{aa} Indiana University, Bloomington, IN 47405, USA

^{ab} INFN Laboratori Nazionali di Frascati, I-00044, Frascati, Italy

^{ac} INFN Laboratori Nazionali di Frascati, INFN Sezione di Perugia, I-06100, Perugia, Italy

^{ad} INFN Laboratori Nazionali di Frascati, University of Perugia, I-06100, Perugia, Italy

^{ae} INFN Sezione di Ferrara, I-44122, Ferrara, Italy

^{af} INFN Sezione di Ferrara, University of Ferrara, I-44122, Ferrara, Italy

^{ag} Institute of Modern Physics, Lanzhou 730000, People's Republic of China

^{ah} Institute of Physics and Technology, Peace Avenue 54B, Ulaanbaatar 13330, Mongolia

^{ai} Instituto de Alta Investigación, Universidad de Tarapacá, Casilla 7D, Arica, Chile

^{aj} Jilin University, Changchun 130012, People's Republic of China

^{ak} Johannes Gutenberg University of Mainz, Johann-Joachim-Becher-Weg 45, D-55099 Mainz, Germany

^{al} Joint Institute for Nuclear Research, 141980 Dubna, Moscow region, Russia

^{am} Justus-Liebig-Universitaet Giessen, II. Physikalisches Institut, Heinrich-Buff-Ring 16, D-35392 Giessen, Germany

^{an} Lanzhou University, Lanzhou 730000, People's Republic of China

^{ao} Liaoning Normal University, Dalian 116029, People's Republic of China

^{ap} Liaoning University, Shenyang 110036, People's Republic of China

^{ad} Nanjing Normal University, Nanjing 210023, People's Republic of China

^{ar} Nanjing University, Nanjing 210093, People's Republic of China

^{as} Nankai University, Tianjin 300071, People's Republic of China

^{at} National Centre for Nuclear Research, Warsaw 02-093, Poland

^{au} North China Electric Power University, Beijing 102206, People's Republic of China

^{av} Peking University, Beijing 100871, People's Republic of China

^{aw} Qufu Normal University, Qufu 273165, People's Republic of China

^{ax} Shandong Normal University, Jinan 250014, People's Republic of China

^{ay} Shandong University, Jinan 250100, People's Republic of China

^{az} Shanghai Jiao Tong University, Shanghai 200240, People's Republic of China

^{ba} Shanghai Jiao Tong University, Shanghai 200240, People's Republic of China

^{bb} Shanxi Normal University, Linfen 041004, People's Republic of China

^{bc} Sichuan University, Chengdu 610064, People's Republic of China

^{bd} Soochow University, Suzhou 215006, People's Republic of China

^{be} South China Normal University, Guangzhou 510006, People's Republic of China

^{bf} Southeast University, Nanjing 211100, People's Republic of China

^{bg} State Key Laboratory of Particle Detection and Electronics, Beijing 100049, Hefei 230026, People's Republic of China

^{bi} Sun Yat-Sen University, Guangzhou 510275, People's Republic of China

^{bj} Suranaree University of Technology, University Avenue 111, Nakhon Ratchasima 30000, Thailand

^{bj} Tsinghua University, Beijing 100084, People's Republic of China

^{bk} Turkish Accelerator Center Particle Factory Group, Istinye University, 34010, Istanbul, Turkey

^{bl} Turkish Accelerator Center Particle Factory Group, Near East University, Nicosia, North Cyprus, 99138, Mersin 10, Turkey
^{bm} University of Chinese Academy of Sciences, Beijing 100049, People's Republic of China
^{bn} University of Groningen, NL-9747 AA Groningen, the Netherlands
^{bo} University of Hawaii, Honolulu, HI 96822, USA
^{bp} University of Jinan, Jinan 250022, People's Republic of China
^{bd} University of Manchester, Oxford Road, Manchester, M13 9PL, United Kingdom
^{br} University of Muenster, Wilhelm-Klemm-Strasse 9, 48149 Muenster, Germany
^{bs} University of Oxford, Keble Road, Oxford OX13RH, United Kingdom
^{bt} University of Science and Technology Liaoning, Anshan 114051, People's Republic of China
^{bu} University of Science and Technology of China, Hefei 230026, People's Republic of China
^{bv} University of South China, Hengyang 421001, People's Republic of China
^{bw} University of the Punjab, Lahore-54590, Pakistan
^{bx} University of Turin and INFN, I-10125, Turin, Italy
^{by} University of Turin and INFN, University of Eastern Piedmont, I-15121, Alessandria, Italy
^{bz} University of Turin and INFN, I-10125, Turin, Italy
^{ca} Uppsala University, Box 516, SE-75120 Uppsala, Sweden
^{cb} Wuhan University, Wuhan 430072, People's Republic of China
^{cc} Xinyang Normal University, Xinyang 464000, People's Republic of China
^{cd} Yantai University, Yantai 264005, People's Republic of China
^{ce} Yunnan University, Kunming 650500, People's Republic of China
^{cf} Zhejiang University, Hangzhou 310027, People's Republic of China
^{cg} Zhengzhou University, Zhengzhou 450001, People's Republic of China

ARTICLE INFO

Article history:

Received 26 May 2023
 Received in revised form 28 September 2023
 Accepted 6 October 2023
 Available online 17 October 2023
 Editor: M. Doser

Keywords:
 Charmed meson
 Spin and parity
 BESIII

ABSTRACT

The spin and parity of the charmed mesons D_s^{*+} , D^{*0} and D^{*+} are determined for the first time to be $J^P = 1^-$ with significances greater than 10σ over other hypotheses of 2^+ and 3^- , using an e^+e^- collision data sample with an integrated luminosity of 3.19 fb^{-1} collected by the BESIII detector at a center-of-mass energy of 4.178 GeV . Different spin-parity hypotheses are tested via a helicity amplitude analysis of the processes $e^+e^- \rightarrow D_s^{*+}D_s^-$, $D^{*0}\bar{D}^0$ and $D^{*+}D^-$, with $D_s^{*+} \rightarrow D_s^+\gamma$, $D^{*0} \rightarrow D^0\pi^0$, and $D^{*+} \rightarrow D^+\pi^0$. The results confirm the quark model predictions.

© 2023 The Author(s). Published by Elsevier B.V. This is an open access article under the CC BY license (<http://creativecommons.org/licenses/by/4.0/>). Funded by SCOAP³.

1. Introduction

Charmed-meson spectroscopy provides a powerful tool to achieve a better understanding of the strong interaction. Following the experimental discovery of the D^+ meson [1], first predictions of the charmed meson spectrum from the quark model emerged in the 1980s [2]. Although the quark model has successfully predicted masses and spin-parity assignments, experimental confirmations are in many places still missing. Notably, the supposed assignment of D_s^{*+} , D^{*0} and D^{*+} as states with quantum numbers $J^P = 1^-$ [3–7] has not yet been confirmed by any experiment. The Particle Data Group (PDG) labels J^P of the D_s^{*+} meson as ‘unknown’ [3], the only experimental measurement [8] found a spin of 1 for the D^{*0} , ruling out spin 0. The observed decay modes $D_{(s)}^* \rightarrow D_{(s)}\pi$ rule out unnatural spin-parity assignments, *i.e.* 1^+ , 2^- , or 3^+ . The hypotheses 1^- , 2^+ , and 3^- remain to be tested.

Over the past decade, charmed-meson spectroscopy has undergone a resurgence due to the discovery of numerous excited charm and charm-strange meson states by the BaBar [9–13], Belle [9,14], CLEO [15] and LHCb [16] collaborations. The observation of these new resonances has provided essential knowledge about the radial excitations ($2S$) and orbital excitations with angular momenta $L = 1$ and 2. The knowledge of spin and parity of the $D_{(s)}^*$ is vital to determine the quantum numbers of higher excited $D_{(s)}^{**}$ states that are reconstructed via $D_{(s)}^*$ mesons. Recently, the first candidates for a hidden-charm tetraquark with strangeness, $Z_{cs}(3985)^+$ [17] and $Z_{cs}(3985)^0$ [18] were observed by BESIII in their decays to the final states $(D_s^-D^{*0} + D_s^+D^0)$ and $(D_s^+D^{*-} + D_s^{*+}D^-)$. Hence, the

spin and parity of the D^{*0} and D_s^{*+} are essential to determine the quantum numbers of $Z_{cs}(3985)^+$.

In this Letter, the spin-parity quantum numbers of D_s^{*+} , D^{*0} , and D^{*+} mesons are determined using a data set with an integrated luminosity of 3.19 fb^{-1} collected with the BESIII detector at the center-of-mass (CM) energy of 4.178 GeV . The spin-parity hypotheses 1^- , 2^+ , and 3^- are tested by means of the helicity amplitude analysis of $e^+e^- \rightarrow D_s^{*+}D_s^-$, $D^{*0}\bar{D}^0$, $D^{*+}D^-$ processes, with $D_s^{*+} \rightarrow D_s^+\gamma$, $D^{*0} \rightarrow D^0\pi^0$, and $D^{*+} \rightarrow D^+\pi^0$ final states. Throughout this letter, charge conjugation is implied, unless explicitly stated otherwise. A partial reconstruction technique is adopted, namely, one $D_{(s)}$ and $\pi^0(\gamma)$ particles are detected to identify the $D_{(s)}^*$ decay, while the other $D_{(s)}$ in the event is undetected. The $D_{(s)}^*$ candidates are reconstructed in the hadronic decay modes $D_s^* \rightarrow K_S^0K^+$, $D^0 \rightarrow K^-\pi^+$, and $D^+ \rightarrow K^-\pi^+\pi^+$ processes. The intermediate states K_S^0 and π^0 are reconstructed via their decays to $\pi^+\pi^-$ and $\gamma\gamma$ final states, respectively.

2. BESIII detector and Monte Carlo simulation

The BESIII detector [19] records symmetric e^+e^- collisions provided by the BEPCII storage ring [20], which operates in the CM energy range from 2.0 GeV to 4.946 GeV , where BESIII has collected large data samples [21]. The cylindrical core of the BESIII detector covers 93% of the full solid angle and consists of a helium-based multilayer drift chamber (MDC), a time-of-flight system (TOF) using plastic scintillators in the central region (barrel) and multi-gap RPCs in the end caps, and a CsI(Tl) electromagnetic calorimeter (EMC), which are all enclosed in a superconducting solenoidal magnet providing a 1.0 T magnetic field. The solenoid is supported

by an octagonal flux-return yoke instrumented with resistive plate counter muon identification modules interleaved with steel. The charged-particle momentum resolution at $1\text{ GeV}/c$ is 0.5%, and the specific ionization energy loss (dE/dx) resolution is 6% for electrons from Bhabha scattering. The EMC measures photon energies with a resolution of 2.5% (5%) at 1 GeV in the barrel (end cap) region. The time resolution in the TOF barrel region is 68 ps, while that in the end cap region is 60 ps [22].

Simulated data samples are produced with a GEANT-4 [23] based Monte Carlo (MC) package, which includes the geometric description [24] of the BESIII detector and the detector response, are used to determine detection efficiencies and to estimate backgrounds. The simulation includes the beam energy spread and initial state radiation in the e^+e^- annihilations modeled with the event generator KKMC [25]. An MC sample of inclusive decays, forty times larger than the data set, includes the production of open charm processes, the initial state radiation production of vector charmonium(-like) states, and the continuum processes. The known decay modes are modeled with EVTGEN [26] using branching fractions taken from the PDG [3], and the remaining unknown charmonium decays are modeled with LUNDCHARM [27]. Final state radiation (FSR) from charged final state particles is incorporated using PHOTOS [28]. MC samples of $e^+e^- \rightarrow \pi^0(\gamma)D_{(s)}D_{(s)}$, simulated following a three-body phase space (PHSP) distribution, are used to determine the selection efficiency. In these simulations, one of the $D_{(s)}$ mesons decays inclusively, based on the branching fractions listed in PDG, and the second one decays to the signal final states.

3. Event selection

To select the signal candidates of the analyzed processes $e^+e^- \rightarrow D_s^{*+}D_s^- \rightarrow \gamma D_s^+D_s^-$, $e^+e^- \rightarrow D^{*0}\bar{D}^0 \rightarrow \pi^0D^0\bar{D}^0$, and $e^+e^- \rightarrow D^{*+}D^- \rightarrow \pi^0D^+D^-$, the selection criteria described below are implemented. The decay modes of $D_{(s)}$ used for reconstruction are $D_s^+ \rightarrow K_S^0K^+$, $D^0 \rightarrow K^-\pi^+$ and $D^+ \rightarrow K^-\pi^+\pi^+$.

The distance of closest approach of each charged track to the e^+e^- interaction point (IP) is required to be within 10 cm along the beam direction and within 1 cm in the plane perpendicular to the beam direction, except for the tracks from K_S^0 decays. The polar angle θ between the direction of a charged track and the positron beam must satisfy $|\cos\theta| < 0.93$ for an effective measurement in the active volume of the MDC. The dE/dx information recorded by the MDC and the time-of-flight information measured by the TOF are used to identify particles by calculating the probabilities \mathcal{P} for various particle hypotheses. Charged kaons and pions are identified requiring $\mathcal{P}(K) > \mathcal{P}(\pi)$ and $\mathcal{P}(\pi) > \mathcal{P}(K)$, respectively.

Shower clusters in the EMC without associated charged tracks are identified as photon candidates if the deposited energy is greater than 25 MeV in the barrel region ($|\cos\theta| < 0.80$) or greater than 50 MeV in the endcap region ($0.86 < |\cos\theta| < 0.92$). To suppress background from electronic noise and coincidental EMC showers, the difference between the event start time and the EMC signal is required to be smaller than 700 ns. The π^0 candidates are reconstructed from photon pairs with an invariant mass $M(\gamma\gamma)$ within $[0.115, 0.150]\text{ GeV}/c^2$.

The K_S^0 candidates are reconstructed from two oppositely charged tracks, without a particle identification (PID) requirement. These tracks are required to originate at a common decay vertex (with a vertex χ^2 less than 100) lying within a distance of 20 cm from the interaction point along the beam direction, accounting for the long lifetime of the K_S^0 meson. Furthermore, the decay vertex is required to be separated from the IP by a distance of at least twice the fitted vertex resolution. The invariant mass of $\pi^+\pi^-$ pairs, $M(\pi^+\pi^-)$, is required to be in the range $[0.487, 0.511]\text{ GeV}/c^2$.

The purity of the selected sample is improved by various constraints listed in Table 1, involving the invariant mass $M(D_{(s)})$ of the reconstructed $D_{(s)}$ meson and the energy difference ΔE between the total energy of the $\pi^0(\gamma)D_{(s)}D_{(s)}$ system in the CM frame and the CM energy E_0 . The applied constraints correspond to three times the resolution of the respective observables,

$$\Delta E = E_{D_{(s)}} + E_{\pi^0(\gamma)} + E_{\text{rec}} - E_0, \quad (1)$$

where $E_{D_{(s)}}$ and $E_{\pi^0(\gamma)}$ are the energies of reconstructed $D_{(s)}$ and $\pi^0(\gamma)$ from $D_{(s)}^*$ candidates, respectively, and E_{rec} is the energy of the recoil side, defined as

$$E_{\text{rec}} = \sqrt{\left| \vec{p}_{D_{(s)}} + \vec{p}_{\pi^0(\gamma)} \right|^2 c^2 + m_{D_{(s)}}^2 c^4}, \quad (2)$$

where $\vec{p}_{D_{(s)}}$ is the total momentum of the reconstructed $D_{(s)}$ meson, $\vec{p}_{\pi^0(\gamma)}$ is the momentum of the $\pi^0(\gamma)$ from $D_{(s)}^*$, and $m_{D_{(s)}}$ is the known mass of the $D_{(s)}$ meson [3]. For each decay mode with multiple $D_{(s)}\pi^0(\gamma)$ candidates in an event, the one with the minimal $|\Delta E|$ is selected.

In order to suppress background contributions and to improve the momentum resolution, a kinematic fit is performed for the three processes. In the case of the $\gamma D_s^+D_s^-$ decay mode, the invariant mass of $K_S^0K^+$ system is constrained to the known D_s^+ mass, and the recoil $D_s^+\gamma$ mass is constrained to the known D_s^- mass. After the kinematic fit, the four-momenta of all final state particles are updated for further analyses.

Fig. 1 shows two-dimensional distribution of the $D_{(s)}^*$ invariant mass, $M(D_{(s)}\pi^0(\gamma))$, and the $D_{(s)}$ recoil mass, $M_R(D_{(s)})$, where two structures are evident. Taking Fig. 1(a) as an example, the horizontal band represents the $e^+e^- \rightarrow D_s^{*+}D_s^-$ process, while the vertical band represents the $e^+e^- \rightarrow D_s^{*-}D_s^+$ process. For the subsequent analysis, only events located in regions of the horizontal or vertical bands defined in Table 1, also illustrated in Fig. 1, are retained. In addition, events in the region common to the horizontal and vertical bands are rejected, since it is impossible to determine whether they stem from the $e^+e^- \rightarrow D_s^{*+}D_s^-$ or the $e^+e^- \rightarrow D_s^+D_s^{*-}$ process. Here, the horizontal band is defined as D_s^{*+} -tag sample and the vertical band is defined as D_s^+ -recoil sample. The background events are studied with the inclusive MC, and the background contamination is determined to be less than 8%. These two data samples are used to perform the helicity amplitude analysis. Similar selection procedures are also applied to D^{*0} and D^{*+} .

4. Formalism

To examine the implications of the spin and parity of the D_s^{*+} , D^{*0} , and D^{*+} , the helicity formalism [29,30] is applied to the analysis of the joint angular distribution for charmed mesons and their daughter particles. Fig. 2 shows the helicity frame for the $e^+e^- \rightarrow D_s^{*+}D_s^-$ process. The helicity angle θ_0 is defined as the angle between the D_s^{*+} momentum and the e^+ beam axis in the CM system. The helicity angles θ_1 and ϕ_1 are related to the decay $D_s^{*+} \rightarrow D_s^+\gamma$. The former is defined as the angle between the D_s^+ momentum in the D_s^{*+} rest frame and the D_s^{*+} momentum in the CM frame, and the latter as the angle between the D_s^{*+} production and decay planes.

For a two-body decay, $A(J, m) \rightarrow B(s, \lambda)C(\sigma, \nu)$, the helicity amplitude $F_{\lambda, \nu}^J$ is related to the covariant amplitude via [31–33]

$$F_{\lambda, \nu}^J = \sum_{LS} \sqrt{\frac{2L+1}{2J+1}} \langle L0, S\delta | J, \delta \rangle \langle s\sigma, \lambda - \nu | S, \delta \rangle g_{LS} r^L \frac{B_L(r)}{B_L(r_0)}, \quad (3)$$

where $\delta = \lambda - \nu$, $\langle \dots \rangle$ are the Clebsch-Gordan Coefficients, g_{LS} is the LS -coupling constant, S the total spin, L the orbital angular

Table 1
Requirements on ΔE , $M(D_{(s)})$, $M(D_{(s)}\pi^0(\gamma))$ and $M_R(D_{(s)})$ for each data sample.

Data sample	ΔE (MeV)	$M(D_{(s)})$ (MeV/c ²)	$M(D_{(s)}\pi^0(\gamma))$ (MeV/c ²)	$M_R(D_{(s)})$ (MeV/c ²)
D_s^{*+} -tag	(−20, 30)	(1950, 1990)	(2105, 2120)	⟨2095, 2135⟩
D_s^+ -recoil			⟨2095, 2135⟩	(2105, 2120)
D^{*0} -tag	(−30, 30)	(1840, 1890)	(2005, 2009)	(2010, 2090)
D^0 -recoil			(2010, 2090)	(2005, 2009)
D^{*+} -tag	(−20, 20)	(1850, 1890)	(2008.5, 2012.5)	(2010, 2090)
D^+ -recoil			(2010, 2090)	(2008.5, 2012.5)

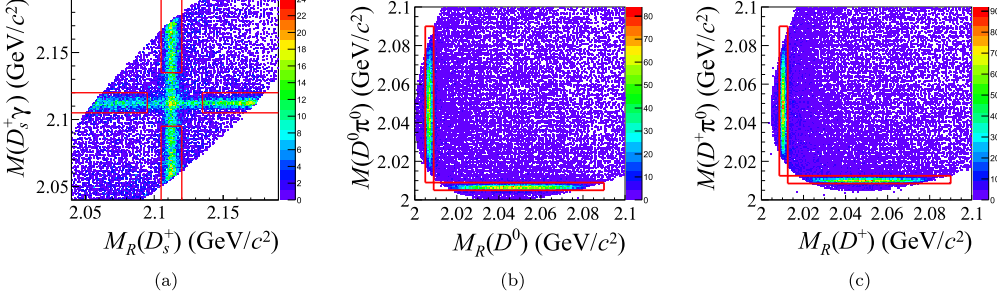


Fig. 1. Two-dimensional distributions of $M(D_{(s)}\pi^0(\gamma))$ and $M_R(D_{(s)})$, where the red rectangle denotes the signal region.

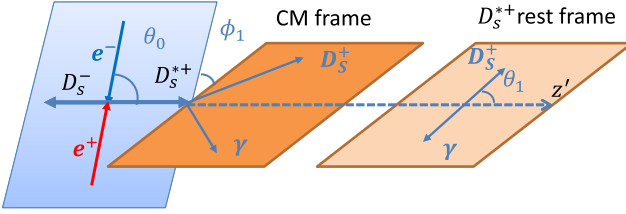


Fig. 2. Definition of the helicity frame for $e^+e^- \rightarrow \gamma^* \rightarrow D_s^{*+}D_s^-$, $D_s^{*+} \rightarrow \gamma D_s^+$ sequential decay.

momentum. The Blatt-Weisskopf factor [34] is represented by B_L , and $r = |\vec{p}_B - \vec{p}_C|$ is the modulus of 3-vector momentum difference between the two final state particles, and r_0 corresponds to choice by setting resonant invariant mass equal to its nominal mass.

The process $e^+e^- \rightarrow \gamma^* \rightarrow D_s^{*+}(\lambda_R)D_s^-$, $D_s^{*+} \rightarrow \gamma(\lambda_1)D_s^+$ is discussed for illustration. The D_s^{*+} meson is assigned spin J and helicity λ_R , the decay photon and the virtual photon γ^* have helicities λ_1 and m , respectively. Then the joint amplitude is

$$A(m, \lambda_1, \vec{\omega}) = \sum_{\lambda_R} F_{\lambda_R, 0} D_{m, \lambda_R}^{1*}(\phi_0, \theta_0, 0) \\ BW(m_{12}) F_{0, \lambda_1}^J D_{\lambda_R, -\lambda_1}^{J*}(\phi_1, \theta_1, 0), \quad (4)$$

where $\vec{\omega} = (\theta_0, \phi_0, \theta_1, \phi_1, m_{12})$, $D_{m, \lambda}^J(\phi, \theta, 0)$ is the Wigner-D function, BW denotes the Breit-Wigner function, m_{12} is the γD_s^+ invariant mass, and $F_{\lambda_R, 0}$ and F_{0, λ_1}^J are the helicity amplitudes of the two sequential decays. The decay amplitude for the D_s^{*0} and D_s^{*+} mesons can be constructed analogously. Then the differential cross section of the sequential decay via D_s^* is

$$\mathcal{W}^{J^P}(\theta_0, \theta_1, \phi_1, m_{12}) = \sum_{m, \lambda_1} |A(m, \lambda_1, \vec{\omega})|^2, \quad (5)$$

with summation over $m = \pm 1$ for the virtal photon, corresponding to the diagonal γ^* spin density matrix $\text{diag}\{1, 0, 1\}$ and $\lambda_1 = \pm 1$ for the radiative photon.

5. Significance estimation

The spin-parity hypotheses are tested using the likelihood function,

$$\mathcal{L}^{J^P}(N) = \prod_{i=1}^N \frac{1}{C} \mathcal{W}^{J^P}(\theta_0^i, \theta_1^i, \phi_1^i, m_{12}^i), \quad (6)$$

where N is the number of selected events, $(\theta_0^i, \theta_1^i, \phi_1^i)$ are the helicity angles for the i -th event describing the D_s^* decay, and \mathcal{W}^{J^P} is the differential cross section of the sequential decay. The normalization factor $C = \int \mathcal{W}^{J^P}(\theta_0^i, \theta_1^i, \phi_1^i, m_{12}) d\cos\theta_0 d\cos\theta_1 d\phi_1 dm_{12}$ is numerically evaluated using a phase-space MC sample, but only including the events passing the detector acceptance and final event selection stage in order to also include efficiency effects.

We perform an unbinned maximum likelihood fit to the angular distribution of the selected events in the signal region. The background contributions are subtracted from the log-likelihood values based on selected events in the inclusive MC falling inside the signal region. The MINUIT package [35] is used to minimize the negative net log-likelihood defined by

$$S = -\ln \mathcal{L}^{J^P} = -\alpha [\ln \mathcal{L}^{J^P} - \omega_{\text{bkg}} \ln \mathcal{L}^{J^P}], \quad (7)$$

where N_s (N_b) is the number of events in data and MC samples. The background weight, $\omega_{\text{bkg}} = 0.025$, is the ratio of the integrated luminosities of the data and the MC sample. To achieve an unbiased uncertainty estimation, the normalization factor derived in Ref. [36–38] is taken into account, expressed as

$$\alpha = \frac{N_s - \omega_{\text{bkg}} N_b}{N_s + \omega_{\text{bkg}}^2 N_b}. \quad (8)$$

Fit results for the mass and angular distributions of the $D_{(s)}^*$ -tag sample for the hypotheses $J^P=1^-$ are shown in Fig. 3. Mass and angular distributions of the hypotheses $J^P = 2^+$ and 3^- can be found in the supplemental material [39]. The moment $\langle \sin^2 \theta_1 \rangle$, which represents an average observed in each ϕ_1 bin, is a useful observable illustrating the different behaviors expected for different hypotheses ($J^P = 1^-, 2^+$ and 3^-). Fig. 4 shows the $\langle \sin^2 \theta_1 \rangle$

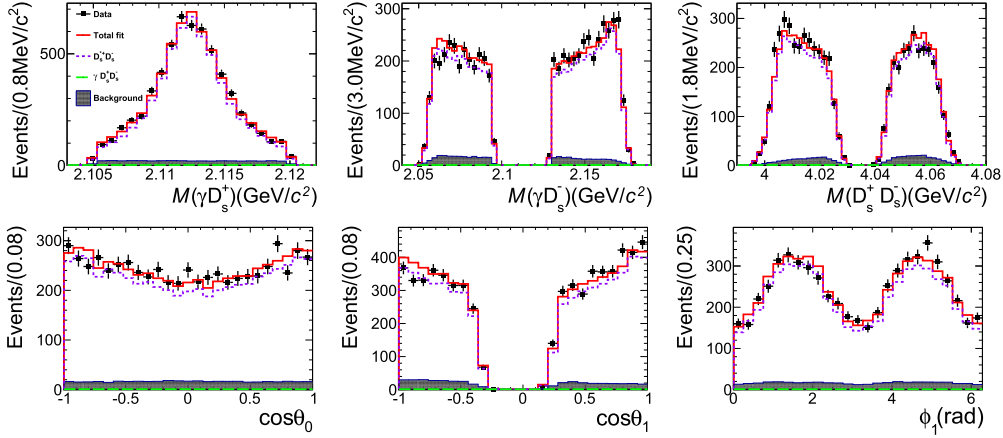


Fig. 3. Mass and angular distributions of D_s^{*+} tag sample for $J^P = 1^-$ hypothesis. Points with error bars are data. The solid red line, dotted purple line, and long dashed green line are the total fit results, $D_s^{*+}D_s^-$, and $\gamma D_s^{*+}D_s^-$ processes, respectively. The shaded black histograms indicate the scaled backgrounds derived from the inclusive MC samples.

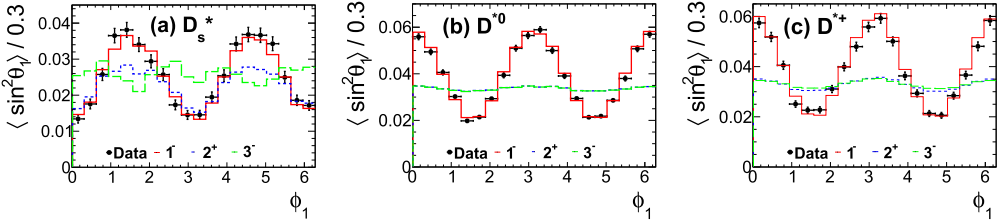


Fig. 4. Distributions of the normalized moment $\langle \sin^2 \theta \rangle / 0.3$ versus ϕ_1 for the processes $e^+e^- \rightarrow$ (a) $D_s^{*+}D_s^-$, (b) $D_s^0\bar{D}^0$ and (c) $D_s^{*+}D^-$. Points with error bars are data summing over D^* -tag sample and D -recoil sample with background events subtracted. The solid red line, dotted blue line, and the long-dashed green line are the fit results for the $J^P = 1^-$, 2^+ , and 3^- hypothesis, respectively. For the (b) and (c) processes, the blue line is hidden below green line.

Table 2

The significance of $J^P = 1^-$ over other quantum number hypotheses. The significance is obtained considering changes in the difference of NDF. In each case that change is $\Delta(\text{NDF}) = 4$, accounting for the mass and width of the D^* and the magnitude and phase for each component. The significance in all cases exceeds 10σ .

Process	Hypothesis	$\Delta(-2 \ln \mathcal{L})$
$D_s^{*+}D_s^-$	1^- over 2^+	1102
	1^- over 3^-	2104
$D_s^0\bar{D}^0$	1^- over 2^+	12134
	1^- over 3^-	12096
$D_s^{*+}D^-$	1^- over 2^+	11308
	1^- over 3^-	11222

distributions for the three spin-parity hypotheses, which combine the $D_{(s)}^*$ -tag sample and the $D_{(s)}$ -recoil sample.

The significances to accept the 1^- hypothesis for D_s^{*+} , D_s^0 , and D_s^{*+} are determined by the continuous test following Refs. [40,41], where the null hypothesis (H_0) represents the J^P of $D_{(s)}^*$ taken as 2^+ or 3^- and the alternative hypothesis (H_1) represents J^P of $D_{(s)}^*$ taken as a linear combination of either $[2^+, 1^-]$ or $[3^-, 1^-]$. The angular fits based on the two hypotheses are performed to data and the likelihood function values are denoted as $\ln(\mathcal{L}_{H_0})$ and $\ln(\mathcal{L}_{H_1})$.

The significance of the $J^P=1^-$ hypothesis is found to be larger than 10σ , based on the change in likelihood ($-2 \ln \mathcal{L}$) and number of degrees of freedom (NDF) listed in Table 2.

6. Systematic uncertainties

The results of the helicity amplitude analysis can be affected by detector effects and analysis procedures. In order to quantify the impact of such systematic effects on this work, dedicated stud-

ies on control samples are performed and corrections for eventual data/MC differences are evaluated.

The sources of systematic uncertainties include the tracking and PID efficiencies for K^\pm and π^\pm , which are studied with control samples of $e^+e^- \rightarrow K^+K^-\pi^+\pi^-$, $K^+K^-K^+K^-$, $K^+K^-\pi^+\pi^-\pi^0$, $\pi^+\pi^-\pi^+\pi^-$, and $\pi^+\pi^-\pi^+\pi^-\pi^0$ events [42]. The photon reconstruction efficiency is studied using $J/\psi \rightarrow \rho^0\pi^0$ events [43]. The K_S^0 reconstruction efficiency is studied with control samples of $J/\psi \rightarrow K^*(892)^\pm K^\mp$, $K^*(892)^\pm \rightarrow K_S^0\pi^\pm$ and $J/\psi \rightarrow \phi K_S^0 K^\mp \pi^\pm$ [44] decays. The π^0 reconstruction efficiency is studied by the double-tag $D\bar{D}$ hadronic decays $D^0 \rightarrow K^-\pi^+$, $K^-\pi^+\pi^+\pi^-$ versus $\bar{D}^0 \rightarrow K^+\pi^-\pi^0$, $K_S^0\pi^0$ [45,46]. According to the efficiency differences determined above, an overall weighting of MC events is performed to match the data events in the fit.

Additionally, inconsistencies between data and MC in the description of the track helix parameters may result in systematic effects. The helix parameters in MC simulations are, therefore, corrected following the procedure described in Ref. [47].

To estimate potential bias due to differences between the data and MC simulation in the selected regions, the distributions of the kinematic variables ΔE and invariant mass $M(D_{(s)})$, $M(D_{(s)}\pi^0(\gamma))$, and $RM(D_{(s)})$ in MC simulations are smeared with Gaussian functions to match the corresponding distributions in the data.

The systematic uncertainty due to the background weight factor (ω_{bkg}) is estimated by setting it to 0. For the non-perfect resolution description, the values of the BW parameters are varied by one standard deviation ($\pm 1\sigma$) from the nominal fit result and the result with the lowest significance is assigned as the systematic uncertainty.

Taking into account all of the systematic uncertainties, the $J^P = 1^-$ hypothesis is always unambiguous and its significance is always greater than 10σ .

7. Summary

The spin and parity of D_s^{*+} , D^{*0} , and D^{*+} mesons are determined in the processes $e^+e^- \rightarrow D_s^{*+}D_s^-$, $D^{*0}\bar{D}^0$, and $D^{*+}D^-$, based on 3.19 fb^{-1} of e^+e^- collision data accumulated at $\sqrt{s} = 4.178 \text{ GeV}$ with the BESIII detector. The application of a helicity amplitude analysis results in a preference of the quantum number $J^P = 1^-$ over the 2^+ and 3^- hypotheses with a significance of more than 10σ , thus confirming the quark model predictions. This is the first experimental determination of the spin and parity of the $D_{(s)}^*$ mesons, which are the cornerstone for the exploration of the properties of heavier charm and beauty mesons [48].

Declaration of competing interest

The authors declare that they have no known competing financial interests or personal relationships that could have appeared to influence the work reported in this paper.

Data availability

The authors do not have permission to share data.

Acknowledgements

The BESIII Collaboration thanks the staff of BEPCII and the IHEP computing center for their strong support. This work is supported in part by National Key R&D Program of China under Contracts Nos. 2020YFA0406400, 2020YFA0406300; National Natural Science Foundation of China (NSFC) under Contracts Nos. 11635010, 11735014, 11835012, 11875262, 11935015, 11935016, 11935018, 11961141012, 12022510, 12025502, 12035009, 12035013, 12061131003, 12175244, 12192260, 12192261, 12192262, 12192263, 12192264, 12192265, 12221005; the Chinese Academy of Sciences (CAS) Large-Scale Scientific Facility Program; the CAS Center for Excellence in Particle Physics (CCEPP); Joint Large-Scale Scientific Facility Funds of the NSFC and CAS under Contract No. U1832207; CAS Key Research Program of Frontier Sciences under Contracts Nos. QYZDJ-SSW-SLH003, QYZDJ-SSW-SLH040; 100 Talents Program of CAS; Fundamental Research Funds for the Central Universities, Lanzhou University, University of Chinese Academy of Sciences; The Institute of Nuclear and Particle Physics (INPAC) and Shanghai Key Laboratory for Particle Physics and Cosmology; ERC under Contract No. 758462; European Union's Horizon 2020 research and innovation programme under Marie Skłodowska-Curie grant agreement under Contract No. 894790; German Research Foundation DFG under Contracts Nos. 443159800, 455635585, Collaborative Research Center CRC 1044, FOR5327, GRK 2149; Istituto Nazionale di Fisica Nucleare, Italy; Ministry of Development of Turkey under Contract No. DPT2006K-120470; National Research Foundation of Korea under Contract No. NRF-2022R1A2C1092335; National Science and Technology fund; National Science Research and Innovation Fund (NSRF) via the Program Management Unit for Human Resources & Institutional Development, Research and Innovation under Contract No. B16F640076; Polish National Science Centre under Contract No. 2019/35/O/ST2/02907; Suranaree University of Technology (SUT), Thailand Science Research and Innovation (TSRI), and National Science Research and Innovation Fund (NSRF) under Contract No. 160355; The Royal Society, UK under Contract No. DH160214; The Swedish Research Council; U.S. Department of Energy under Contract No. DE-FG02-05ER41374.

Appendix A. Supplementary material

Supplementary material related to this article can be found online at <https://doi.org/10.1016/j.physletb.2023.138245>.

References

- [1] I. Peruzzi, M. Piccolo, G.J. Feldman, H.K. Nguyen, J. Wiss, G.S. Abrams, M.S. Alam, A. Boyarski, M. Breidenbach, W.C. Carithers, et al., Phys. Rev. Lett. 37 (1976) 569.
- [2] S. Godfrey, N. Isgur, Phys. Rev. D 32 (1985) 189.
- [3] R.L. Workman, et al., Particle Data Group, PTEP 2022 (2022) 083C01.
- [4] M. Gell-Mann, Phys. Lett. 8 (1964) 214.
- [5] M.K. Gaillard, B.W. Lee, J.L. Rosner, Rev. Mod. Phys. 47 (1975) 277.
- [6] A. De Rujula, H. Georgi, S.L. Glashow, Phys. Rev. D 12 (1975) 147.
- [7] S.L. Glashow, J. Iliopoulos, L. Maiani, Phys. Rev. D 2 (1970) 1285.
- [8] H.K. Nguyen, J. Wiss, G.S. Abrams, M.S. Alam, A. Boyarski, M. Breidenbach, R. DeVoe, J. Dorfan, G.J. Feldman, G. Goldhaber, et al., Phys. Rev. Lett. 39 (1977) 262.
- [9] A.J. Bevan, et al., BaBar Belle Collaborations, Eur. Phys. J. C 74 (2014) 3026.
- [10] P. del Amo Sanchez, et al., BaBar Collaboration, Phys. Rev. D 82 (2010) 111101.
- [11] B. Aubert, et al., BaBar Collaboration, Phys. Rev. Lett. 97 (2006) 222001.
- [12] B. Aubert, et al., BaBar Collaboration, Phys. Rev. D 80 (2009) 092003.
- [13] J.P. Lees, et al., BaBar Collaboration, Phys. Rev. D 91 (2015) 052002.
- [14] J. Brodzicka, et al., Belle Collaboration, Phys. Rev. Lett. 100 (2008) 092001.
- [15] D. Besson, et al., CLEO Collaboration, Phys. Rev. D 68 (2003) 032002.
- [16] S. Chen, Y. Li, W. Qian, Y. Xie, Z. Yang, L. Zhang, Y. Zhang, arXiv:2111.14360 [hep-ex].
- [17] M. Ablikim, et al., BESIII Collaboration, Phys. Rev. Lett. 126 (2021) 102001.
- [18] M. Ablikim, et al., BESIII Collaboration, Phys. Rev. Lett. 129 (2022) 112003.
- [19] M. Ablikim, et al., BESIII Collaboration, Nucl. Instrum. Methods A 614 (2010) 345.
- [20] C.H. Yu, et al., in: Proceedings of IPAC2016, Busan, Korea, 2016.
- [21] M. Ablikim, et al., BESIII Collaboration, Chin. Phys. C 44 (2020) 040001.
- [22] X. Li, et al., Radiat. Detect. Technol. Methods 1 (2017) 13; Y.X. Guo, et al., Radiat. Detect. Technol. Methods 1 (2017) 15; P. Cao, et al., Nucl. Instrum. Methods A 953 (2020) 163053.
- [23] S. Agostinelli, et al., GEANT4 Collaboration, Nucl. Instrum. Methods A 506 (2003) 250–303.
- [24] K.X. Huang, Z.J. Li, Z. Qian, J. Zhu, H.Y. Li, Y.M. Zhang, S.S. Sun, Z.Y. You, Nucl. Sci. Tech. 33 (2022) 142.
- [25] S. Jadach, B.F.L. Ward, Z. Was, Phys. Rev. D 63 (2001) 113009; Comput. Phys. Commun. 130 (2000) 260.
- [26] D.J. Lange, Nucl. Instrum. Methods A 462 (2001) 152; R.G. Ping, Chin. Phys. C 32 (2008) 599.
- [27] J.C. Chen, G.S. Huang, X.R. Qi, D.H. Zhang, Y.S. Zhu, Phys. Rev. D 62 (2000) 034003; R.L. Yang, R.G. Ping, H. Chen, Chin. Phys. Lett. 31 (2014) 061301.
- [28] E. Richter-Was, Phys. Lett. B 303 (1993) 163.
- [29] M. Jacob, G.C. Wick, Ann. Phys. 7 (1959) 404.
- [30] S.U. Chung, <https://doi.org/10.5170/CERN-1971-008>, 1971.
- [31] S.U. Chung, Phys. Rev. D 57 (1998) 431.
- [32] S.U. Chung, Phys. Rev. D 48 (1993) 1225.
- [33] S.U. Chung, J. Friedrich, Phys. Rev. D 78 (2008) 074027.
- [34] E. Santopinto, A. Giachino, Phys. Rev. D 96 (2017) 014014.
- [35] F. James, CERN-D-506, 1994.
- [36] C. Langenbruch, Eur. Phys. J. C 82 (2022) 393.
- [37] L. Kish, Survey Sampling, Wiley Classics Library (Wiley, New York, 1965).
- [38] M. Ablikim, et al., BESIII Collaboration, J. High Energy Phys. 12 (2022) 033.
- [39] See Supplemental Material at xxx for additional analysis information.
- [40] I.V. Narsky, Nucl. Instrum. Methods A 450 (2000) 444.
- [41] Y.S. Zhu, High Energy Phys. Nucl. Phys. 30 (2006) 331.
- [42] M. Ablikim, et al., BESIII Collaboration, Phys. Rev. D 99 (2019) 112005.
- [43] M. Ablikim, et al., BESIII Collaboration, Phys. Rev. D 81 (2010) 052005.
- [44] M. Ablikim, et al., BESIII Collaboration, Phys. Rev. D 92 (2015) 112008.
- [45] M. Ablikim, et al., BESIII Collaboration, Eur. Phys. J. C 76 (2016) 369.
- [46] M. Ablikim, et al., BESIII Collaboration, Chin. Phys. C 40 (2016) 113001.
- [47] M. Ablikim, et al., BESIII Collaboration, Phys. Rev. D 87 (2013) 012002.
- [48] D.M. Asner, et al., Physics at BES-III, Int. J. Mod. Phys. A 24 (2009) S1–794.